SLAC-PUB-2759
June 1981
(T/E)

OBSERVATION OF NEW RESONANT STRUCTURES IN THE NATURAL SPIN-PARITY STRANGE MESON SYSTEM*

D. Aston,[†] R. Carnegie,[‡] W. Dunwoodie,[†] S. Durkin,[†] P. Estabrooks,[‡] T. Fieguth,[†] R. J. Hemingway,[‡] A. Honma,[†a] D. Hutchinson,[†] W. B. Johnson,[†] P. Kunz,[†] T. Lasinski,[†b] D. W. G. S. Leith,[†] L. Levinson,[†] R. McKee,[¶c] A. McPherson,[‡] W. T. Meyer,[†d] G. Oakham,[‡] B. N. Ratcliff,[†] R. Richter,[†a] S. Shapiro,[†] R. Stroynowski,[†e] S. Suzuki,[†f] S. Williams,[†] J. Va'vra.[‡g]

ABSTRACT

High statistics data for the reaction $K^-p \rightarrow K^-\pi^+n$ have been obtained using the LASS spectrometer at SLAC. An energy independent partial wave analysis of these data yields unique $K^-\pi^+$ elastic scattering partial wave amplitudes in the $K\pi$ invariant mass region from 0.7 GeV to 1.8 GeV, and two distinguishable sets of amplitudes between 1.8 GeV and 2.3 GeV. Besides the three "old" K^* resonances [$J^P = 1^-K^*(892)$, $2^+K^*(1430)$, $3^-K^*(1780)$] these partial waves display evidence for a K^* resonance with $J^P = 4^+$ near 2.07 GeV. The energy dependence of the S wave amplitude confirms the existence of a resonant 0^+ state in the 1.4 GeV region [the $\kappa(1500)$], and provides evidence for a new high mass S wave resonance [$\kappa'(1850)$] near 1.85 GeV. Resonant behavior is also observed in the P wave amplitude around 1.7 GeV.

Submitted to Physics Letters B

---

* Work supported by the Department of Energy, contract DE-AC03-76SF00515.
† Stanford Linear Accelerator Center, Stanford University, Stanford, California 94305.
‡ Carleton University, Ottawa, Ontario, Canada K1S 5B6.
¶ National Research Council, Ottawa, Canada K1A ØR6.

We present results from an energy independent partial wave analysis (PWA) of the $K\pi$ system using high statistics 11 GeV/c data on the reaction

$$K^- p \rightarrow K^- \pi^+ n \qquad (1)$$

at small values of momentum transfer. This reaction is dominated by π exchange, and historically has been an important source of information on $K\pi$ elastic scattering, and the natural spin-parity strange mesons [1]. In a previous analysis of the $K\pi$ system using reaction (1) and several other π exchange dominated reactions at 13 GeV/c ($K^+p \rightarrow K^+\pi^+n$, $K^-p \rightarrow K^-\pi^-\Delta^{++}$, $K^+p \rightarrow K^+\pi^-\Delta^{++}$), evidence was presented for the $J^P = 0^+$ $\kappa(1500)$ and, in two out of the four possible solutions, for P wave resonance structure in the 1.65 GeV region [2]. Acceptance limitations restricted that analysis to $K\pi$ masses below 1.8 GeV. In this paper, we present a PWA of new 11 GeV/c data on reaction (1) which extends the measurement of the $K^-\pi^+$ elastic scattering partial waves up to a mass of 2.26 GeV. Our analysis confirms the previous results in the low mass region ($M_{K\pi} < 1600$ MeV) while clearly displaying additional resonant structure at higher masses.

The experiment was performed in the LASS spectrometer at SLAC [3]. The trigger required two or more charged particles to exit the target, as defined by a proportional chamber 54 cm downstream of the target. Events corresponding to reaction (1) were selected from the charge-zero two-prong reactions in this sample by requiring the missing mass recoiling against the outgoing $K^-\pi^+$ system to lie between 0.45 GeV and 1.05 GeV. Events ambiguous with elastic K^-p events and K^0 decay events were explicitly rejected. The final $K^-p \rightarrow K^-\pi^+n$ data sample consisted of 43,000 events in the $K\pi$ invariant mass range from

0.8 GeV to 2.26 GeV, and the small momentum transfer region, $|t'| < 0.2$ GeV^2.(*) With these cuts, the background to reaction (1) was estimated to be $4 \pm 4\%$.

A Monte Carlo program was used to describe effects due to spectrometer acceptance, and event selection criteria. The data were fitted by a maximum likelihood procedure which yields t-channel acceptance corrected $K\pi$ angular moments as a function of the $K\pi$ invariant mass and t'. In these fits the number of LM moments was limited [$L < L_{max}$ and $M < M_{max}$] to the minimum number required to describe the data in each mass region. Because reaction (1) is dominated by π exchange, the prominent (M) moments are those with $M = 0$. These are shown in fig. 1 as a function of $M_{K\pi}$ for a single t' bin, $|t'| < 0.2$ GeV^2. The most prominent structures in the even L moments are due to the leading K^* resonances while clear interference effects can be seen in the odd angular moments.

Following the method of reference [2], we have performed an energy independent $K\pi$ scattering partial wave analysis using spherical harmonic moments of the data. The simple exchange parametrization of reference [2] was found to describe the t' dependence of these data quite well. This method determines the magnitudes and relative phases of the $K\pi \to K\pi$ scattering partial waves (one overall phase cannot be determined). Below 1.2 GeV the S and P waves are known to be elastic [2], so the imposition of elastic unitarity on the S and P

(*) In performing the partial wave analysis below a $K\pi$ mass of 1.6 GeV, events with an $n\pi$ invariant mass less than 1.8 GeV were also removed. This sample is somewhat more restricted than that used in reference [3].

waves is sufficient to fix the overall phase. In the inelastic region above 1.2 GeV, we fix the phase of the leading K^* resonance in each mass region to the Breit-Wigner phase of the associated resonance, allowing small rotations away from the predicted Breit-Wigner phase in order to assure smooth phase variations (see fig. 3).

There are discrete ambiguities inherent in any pseudoscalar-pseudoscalar scattering amplitude analysis. These ambiguities are most readily apparent in the behavior of the imaginary part of the amplitude zeros (Z_i) described by Barrelet [4]. Requiring the solutions to be smooth, it is possible to switch from one solution to another only when the imaginary part of a particular Barrelet zero approaches zero. Since the Wigner condition, combined with the existence of leading resonances, requires all of the Z_i to turn on with negative imaginary parts, elastic unitarity leads to a unique solution below 1.2 GeV. It is seen in fig. 2 that ambiguities do not arise until $\mathrm{Im}(Z_3)$ approaches zero in the 1.8 GeV region. In the region between 1.9 and 2.0 GeV, $\mathrm{Im}(Z_1)$ is also nearly zero. Thus, we extract a unique solution below 1.8 GeV, two solutions in the region between 1.8 and 2.0 GeV, and four solutions above 2.0 GeV. The definitions of these four solutions in terms of the signs of the imaginary parts of the amplitude zeros in each mass region can be found in table 1.

The $K^-\pi^+$ partial wave magnitudes and phases are shown in fig. 3. In general, these results are consistent with previous measurements, but are of higher statistical significance, particularly in the region above the $K^*(1430)$. The four high mass solutions presented actually fall into only two distinct groups, (A, C) and (B, D) based primarily on the behavior of the S, P and D waves. Both the F and G waves appear insensitive to the solution chosen.

Figure 4 shows the Argand diagrams of the two distinct solution types (A, B). All solutions display the leading $J^P = 1^-, 2^+, 3^-$ and 4^+ resonances as counter clockwise loops in the appropriate Argand diagrams. In particular, the new $J^P = 4^+ K^*(2070)$ [3,5] is indicated by the G wave loop in the 2.1 GeV region. Clear resonance loops are also seen in the S and P waves in the mass region between 1.3 and 1.9 GeV, while the D wave shows an intriguing cusp in the region above the $K^*(1430)$ whose precise interpretation is unclear.

In the S wave solutions at low mass, significant departures from the unitary circle can be seen. These departures are due to the fact that the partial waves presented are the sum of the different isospin parts $a_L = 2/3 \left(a_L^{1/2} + 1/2\ a_L^{3/2}\right)$. The $I = 3/2$ component has been well measured up to 1.6 GeV and contains no significant waves other than the S wave. Above 1.6 GeV, little $I = 3/2$ information exists. In the S wave plots of fig. 4, the dotted lines represent our S wave solutions with the isospin 3/2 component subtracted up to 1.6 GeV using the parameterization of reference [2]. The resulting S wave, which now remains within the unitarity circle, exhibits a slow circular motion in the region from 0.8 GeV to 1.3 GeV. Above this mass, the S wave amplitude undergoes a very rapid circular motion with the fastest change occurring in the 1.4 GeV region. Though the precise location of this maximum speed is clearly dependent on our choice of overall phase, as well as nonresonant S wave backgrounds, we conclude that there exists an S wave resonance in this mass region, confirming the 0^+ $\kappa(1500)$ previously reported [2].

Furthermore, in the mass region above 1.6 GeV, all solutions display clear resonance loops in the mass region from 1.8 and 1.9 GeV. We call this new state the $\kappa'(1850)$.

Figure 4 also shows resonance like behavior in the P wave near 1.7 GeV, similar to that observed by Estabrooks et al. in two of four ambiguous solutions [2]. Although, the rapid rise in the P wave amplitude in the 1.6 GeV region combined with a very flat magnitude thereafter may indicate more complex structure, we will assume the behavior to be due to a single resonance.

We have extracted resonance parameters for the leading states by fitting the rising edge of the associated partial wave magnitude to a relativistic Breit-Wigner resonance form with a Blatt-Weisskopf barrier factor [6]. In performing these fits, we have assumed that the turn-on of the partial waves associated with these states is resonance dominated. The resulting masses, widths, and elasticities are given in table 2.

Faced with sizable nonresonant backgrounds, the overall phase uncertainty, and no clear theoretical understanding of resonance poles, we have not attempted to determine the parameters of the underlying states precisely. Instead, we have estimated their parameters by ascribing circular motion to the Argand diagram resonance loops. The results are shown in table 2. The parameters of the high mass S and P states depend only weakly on the particular solution chosen.

The resonance states observed in these $K^-\pi^+$ partial waves naturally fit into the framework expected from SU(3) and a simple quark model. The $K^*(892)$, $K^*(1430)$, $K^*(1780)$ and $K^*(2070)$ form an L-excitation ladder ($q\bar{q}$ total spin $S = 1$) with L increasing from 0 to 3. The lower 0^+ state at $\sim$ 1400 MeV is naturally classified as the lowest lying member of the L = 1, S =1 $K^*(1430)$ triplet, while the higher 0^+ state would be the first radially excited recurrence. The 1^- resonant behavior at 1700 MeV could be either the L = 0, S = 1 radial recurrence of the $K^*(892)$, the lowest lying member of the L = 2, S = 1 $K^*(1780)$ triplet, or perhaps a superposition of both. Accurate measurements of this invariant mass region in inelastic decay channels may make it possible to establish which of these possibilities is correct.

ACKNOWLEDGEMENTS

We are very grateful for the excellent support we have received from the technical staffs of SLAC Group B, LASS Operations, Carleton University, and the National Research Council. Special thanks are due R. Bierce, F. Holst, A. Kilert, D. McShurley, G. Oxoby and W. Walsh for their help throughout the experiment.

REFERENCES

a. Present address: CERN, CH-1211, Geneva 23, Switzerland.

b. Present address: NASA, Ames Research Center, Mountain View, California 94040.

c. Present address: Los Alamos Scientific Laboratory, Los Alamos, New Mexico 87545.

d. Present address: Iowa State University, Ames, Iowa 50011.

e. Present address: California Institute of Technology, Pasadena, California 91125.

f. On leave from Nagoya University, Nagoya, Japan.

g. Present address: Stanford Linear Accelerator Center, Stanford University, Stanford, California 94305.

1. See: R. L. Kelly et al., Particle Data Group, Rev. Mod. Phys. 52 (1980) No. 2, and references therein.
2. P. Estabrooks et al., Nucl. Phys. B133 (1978) 490.
3. D. Aston et al., Phys. Lett. 99B, (1981) 503.
4. E. Barrelet, Nuovo Cimento 8A (1972) 331.
5. W. E. Cleland et al., Phys. Lett. 97B (1980) 465; D. D. Carmony et al., Phys. Rev. D16 (1977) 1251.
6. J. Blatt and V. Weisskopf, Theoretical Nuclear Physics (Wiley, New York, 1952), p. 316, pp. 409-410.

TABLE 1

The Barrelet Zero Solution Classifications

z_i	Solution A	Solution B	Solution C	Solution D	Mass (GeV)
z_1	+	+	+	+	1.30 to 1.86
z_2	−	−	−	−	
z_3	−	−	−	−	
z_1	+	+	+	+	1.86 to 2.02
z_2	−	−	−	−	
z_3	+	−	+	−	
z_4	−	−	−	−	
z_1	−	−	+	+	2.02 to 2.30
z_2	−	−	−	−	
z_3	+	−	+	−	
z_4	−	−	−	−	

TABLE 2

Leading Resonances

J^P	Mass (MeV)	Width (MeV)	Elasticity
1^-	894.6 ± 0.8	49.8 ± 1.2	
2^+	1428 ± 3	98 ± 8	0.43 ± 0.01
3^-	$1753 {}^{+25}_{-18}$	$300 {}^{+170}_{-80}$	0.16 ± 0.01
4^+	$2070 {}^{+100}_{-40}$	$240 {}^{+500}_{-100}$	0.07 ± 0.01

Underlying Resonances

J^P	Mass (MeV)	Width (MeV)	Elasticity
0^+	~ 1400	~ 250	~ 0.85
0^+	~ 1850	~ 250	~ 0.40
1^-	~ 1700	~ 200	~ 0.35

FIGURE CAPTIONS

Figure 1. The $M=0$, acceptance corrected, $K\pi$ angular moments as a function of mass for the small t' region, $|t'| < 0.2$ GeV^2. These moments are calculated in 40 MeV bins below 1.8 GeV, and 80 MeV bins above this mass.

Figure 2. The $K\pi$ amplitude (Barrelet) zeros as a function of mass.

Figure 3. The mass dependence of the $K\pi$ elastic scattering amplitudes. These data were fit in 20 MeV bins below 1.00 GeV, 40 MeV bins from 1.00 GeV to 1.64 GeV, and 80 MeV bins above 1.64 GeV. The solid line represents the phase predicted by a simple Breit-Wigner fit to the leading resonance in the given mass region. The actual phase in each mass region has been fixed to the phase represented by the symbol o. Where error bars are not shown the size of the points plotted is larger than the statistical error associated with the point.

Figure 4. The Argand diagrams for the $K^-\pi^+$ elastic scattering partial wave amplitudes corresponding to solutions A and B. The overall phase has been fixed as in Figure 3. The ticks are marked at 0.2 GeV intervals.

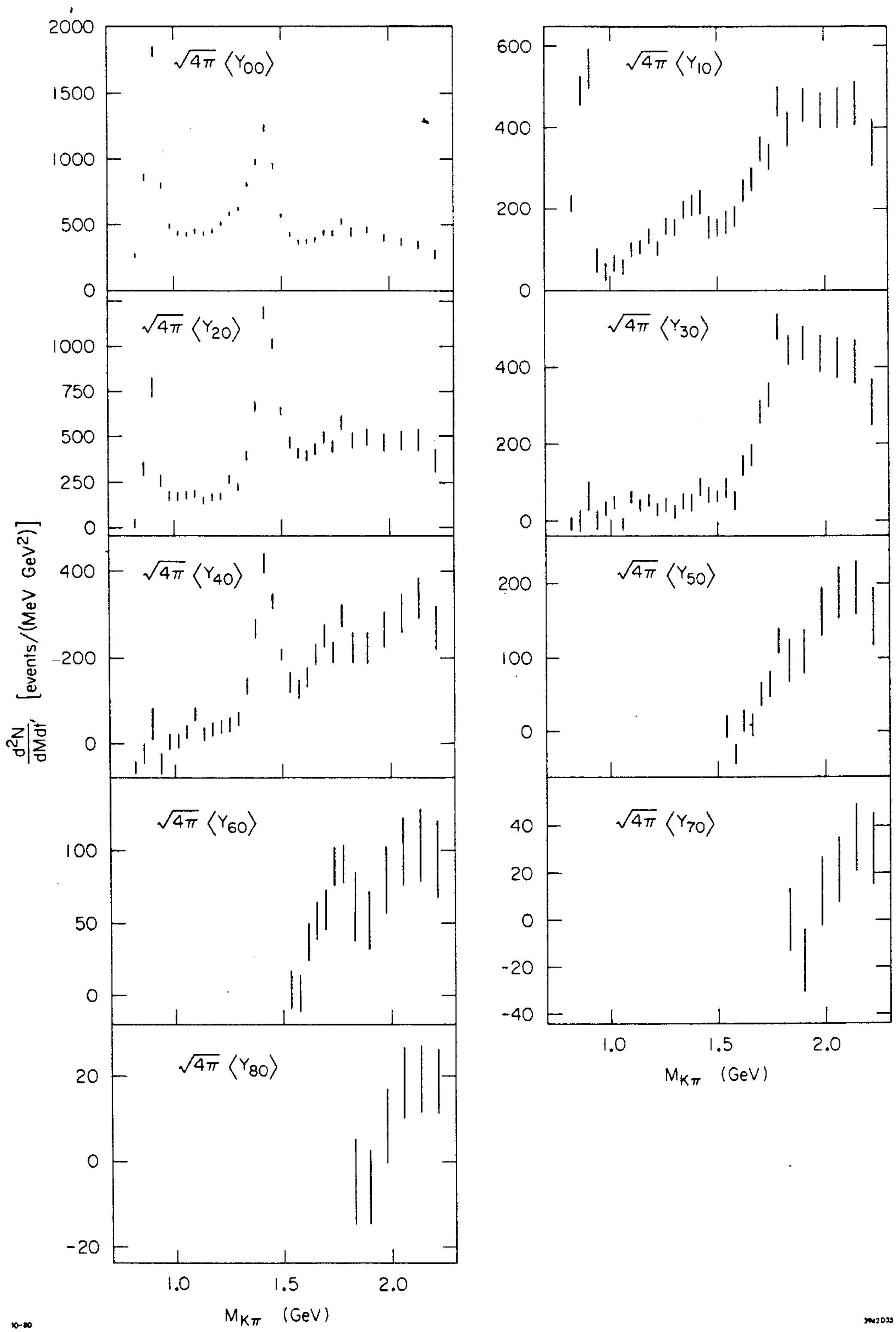
$\sqrt{4\pi}\,\langle Y_{00}\rangle$
$\sqrt{4\pi}\,\langle Y_{10}\rangle$
$\sqrt{4\pi}\,\langle Y_{20}\rangle$
$\sqrt{4\pi}\,\langle Y_{30}\rangle$
$\sqrt{4\pi}\,\langle Y_{40}\rangle$
$\sqrt{4\pi}\,\langle Y_{50}\rangle$
$\sqrt{4\pi}\,\langle Y_{60}\rangle$
$\sqrt{4\pi}\,\langle Y_{70}\rangle$
$\sqrt{4\pi}\,\langle Y_{80}\rangle$
$\frac{d^2N}{dMd\Gamma}$ [events/(MeV GeV^2)]
$M_{K\pi}$ (GeV)
10-80

Fig. 1

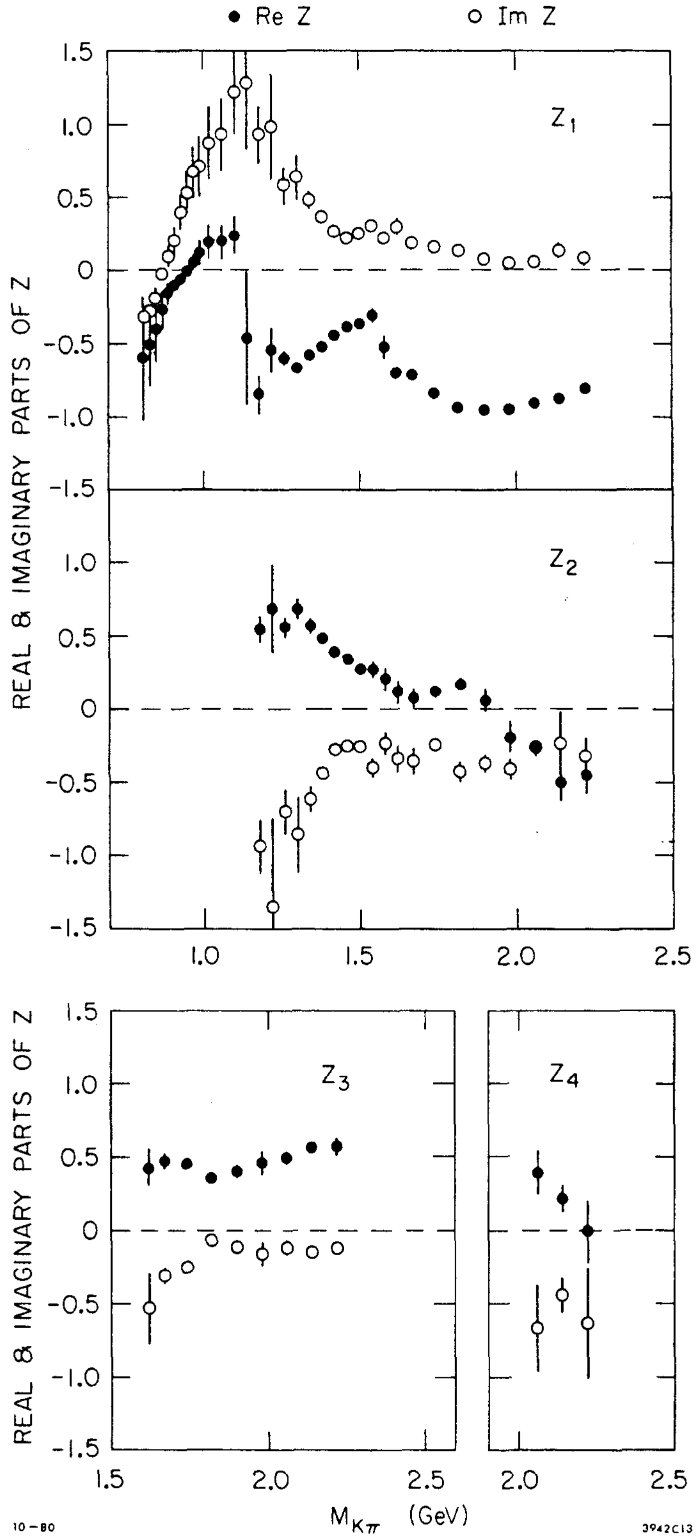

• Re Z
○ Im Z
Z_1
Z_2
Z_3
Z_4
REAL & IMAGINARY PARTS OF Z
$M_{K\pi}$ (GeV)
10-80
3942C13

Fig. 2

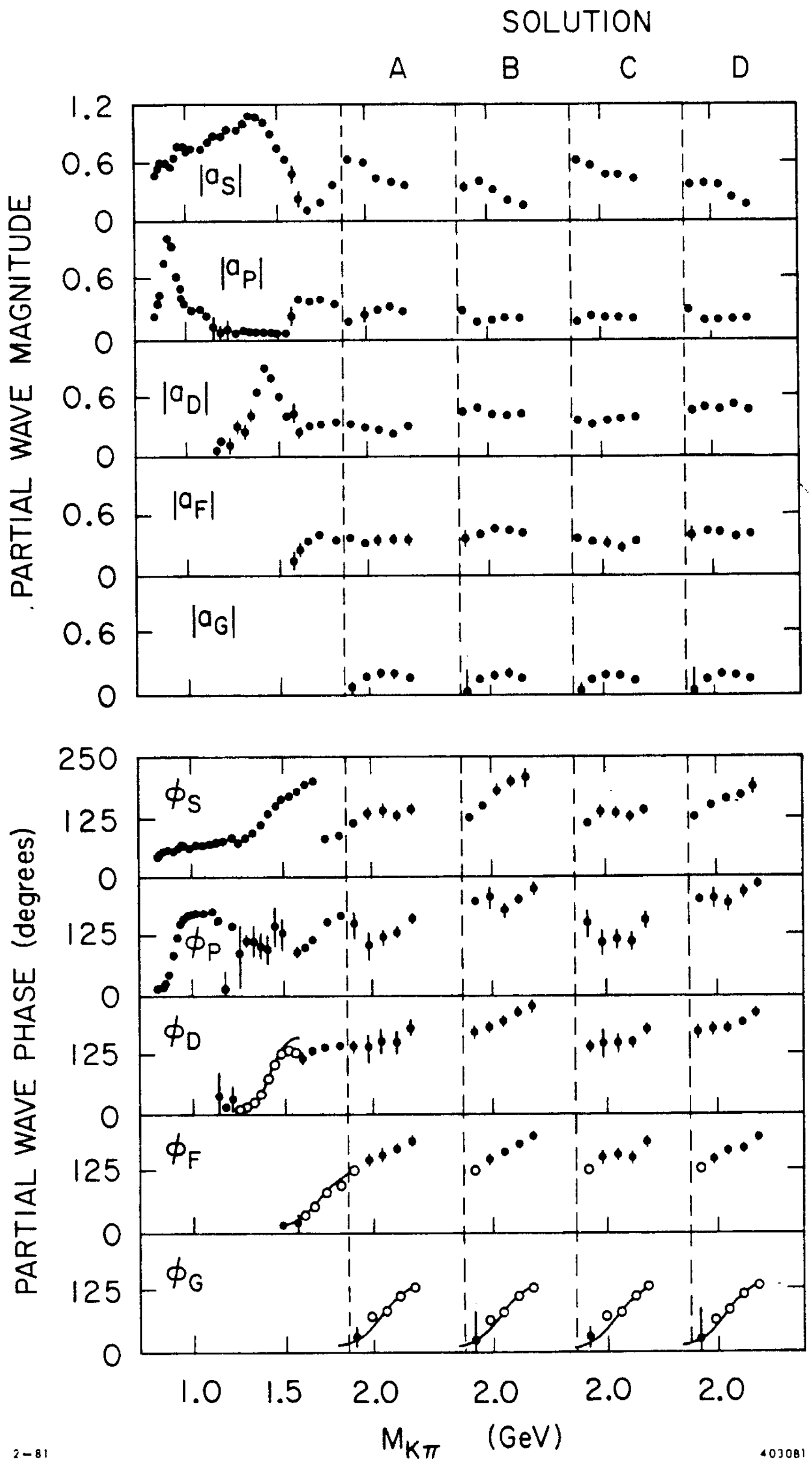
SOLUTION
A
B
C
D
PARTIAL WAVE MAGNITUDE
$|a_S|$
$|a_P|$
$|a_D|$
$|a_F|$
$|a_G|$
1.2
0.6
0
PARTIAL WAVE PHASE (degrees)
250
125
ϕ_S
ϕ_P
ϕ_D
ϕ_F
ϕ_G
1.0
1.5
2.0
$M_{K\pi}$ (GeV)
2-81
403081

Fig. 3

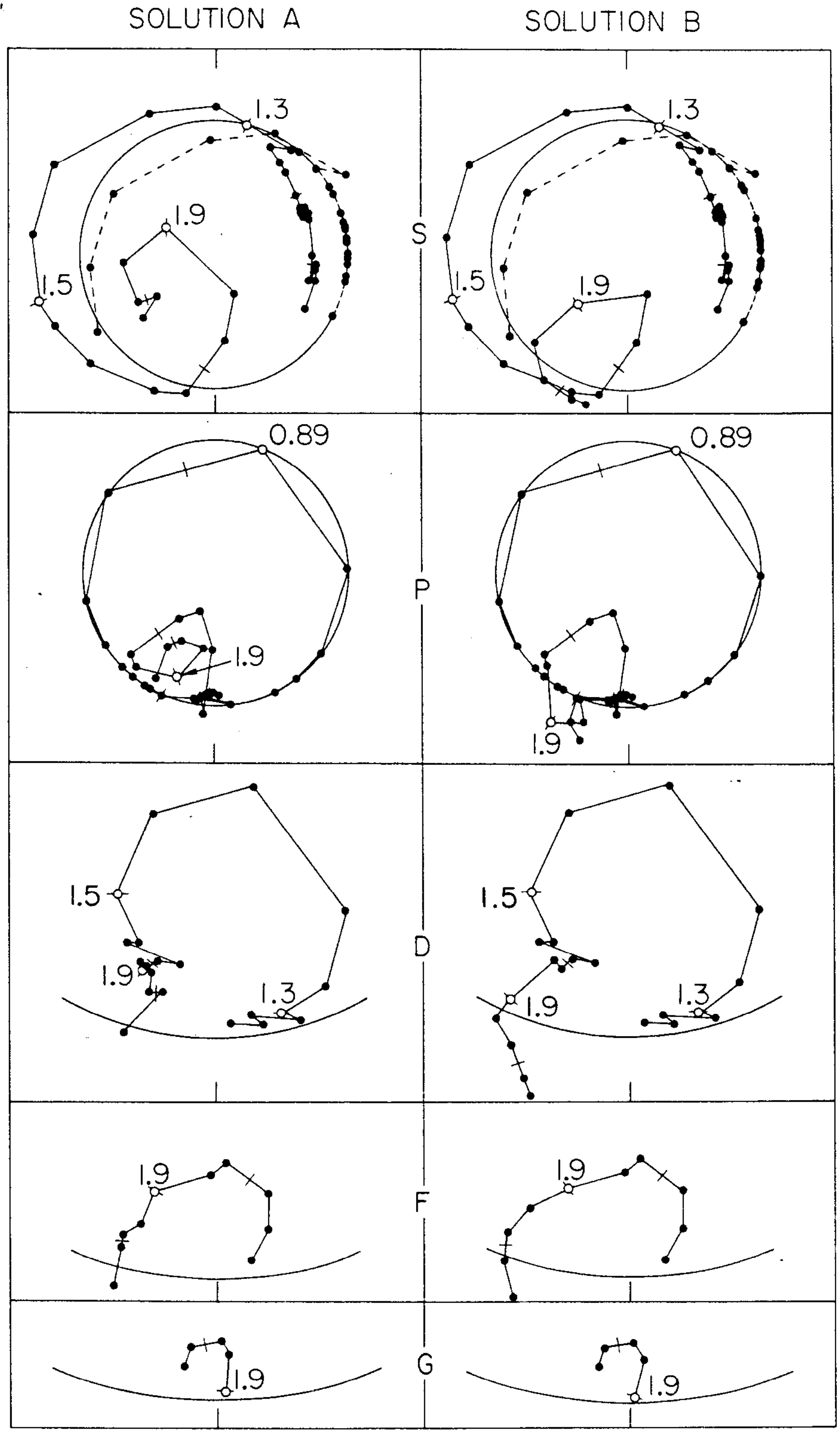

Fig. 4